Rendezvous revisited: The search for fast-intercept solutions

Eric M. Edlund[a)]
Department of Physics, SUNY Cortland, Cortland, New York, 13045

(Received 11 April 2022; accepted 1 June 2023)

Orbital interception scenarios typically involve a chaser that is actively maneuvered to encounter an inertial target and may be undertaken for a variety of purposes, including docking spacecraft or colliding with an asteroid for planetary defense studies. Viable intercept trajectories are constrained by the free-fall path of the target and by auxiliary conditions such as the available time or fuel budget. Whereas a constraint on the time to intercept is central to the (extensively studied) Lambert problem, a less common but more visually compelling constraint is that of the available fuel for intercept. This was the basis of a recent study [E. M. Edlund, Am. J. Phys. **89**, 559–566 (2021)], which analyzed one of the two families of possible intercept solutions that were identified. The second family, studied in more detail here, describes intercepts at all points in the orbit and has the interesting property that it admits fast-intercept solutions. This work concludes the analysis of this problem; it develops a general condition that describes both families of intercepts, presents representative solutions, and considers the sensitivity of these solutions to errors in the control parameters.
https://doi.org/10.1119/5.0095559

I. INTRODUCTION

Long before space travel was considered a possibility, there was great interest in the intercept problem, first made famous by Lambert in 1761. The Lambert problem, as it is now known, seeks the velocity of a body given astronomical measurements of its position at two times. The solution allows the position of the body to be determined at any later time, thereby providing great predictive capability. This problem spurred seminal developments in celestial mechanics and analysis by some of the best minds of the time.[1,2] There is a long and rich history of the literature stemming from the Lambert problem, which was reinvigorated in the 1950s with the development of spaceflight. Modern incarnations of this problem often have a goal of finding the thrust vector that will allow an actively maneuverable craft to intercept an inertial target (meaning a craft on a "free-fall" or "ballistic" path) at a specific time.

A number of recent articles have focused on interesting and insight-building problems involving orbital dynamics, including analysis of the Lambert problem using a search method[3] and using the Hohman transfer in introductory physics courses.[4] An analysis of close-proximity rendezvous using the Clohesy–Wiltshire equations was presented in Ref. 5, a set of multi-thrust methods for achieving escape velocity from an initially circular orbit was given in Ref. 6, and a detailed analysis of Kepler's problem that examines all possible paths between two points in space was provided in Ref. 7. Reference 8 approached the intercept problem by considering a constraint of a specified Δv, which can be thought of as a constraint on the quantity of available fuel. Therefore, it was argued that this particular variation is an excellent problem for undergraduate students, because (in contrast to a constraint on the intercept time) the velocity constraint is more readily visualized and developed deeper intuition for motion on elliptical trajectories. A simple HTML-Javascript simulator was provided to help visualize and gamify this study of orbital dynamics.

While the work of Ref. 5 identified two possible families of intercept solutions, it analyzed only the first family in which intercept/rendezvous occurs after an integer number of chaser orbits. However, the second family of intercept solutions is particularly interesting, because it allows for fast intercepts that occur before the target has completed a full orbit. Such fast-intercept maneuvers may be relevant to planetary defense against civilization-threatening asteroids or comets where a short, but not pre-determined, time may be of the essence.[9] The Planetary Defense Coordination Office, a division within NASA, tracks known threats and develops mitigation plans.[10] As part of that effort, NASA's DART mission successfully intercepted the asteroid Dimorphos, the smaller of a double-asteroid pair, on September 26 of 2022 to test deflection by kinetic impact.[11] Other recent developments in this line of work include space debris collectors[12] and an actively maneuvering Russian satellite thought to be a satellite hunter of sorts.[13]

One can, of course, find solutions to the intercept problem using a "guess-and-check" method, where initial parameters are guessed, the trajectories are checked (using something like the HTML-javascript program distributed with Ref. 5), and then the parameters are iterated until an acceptable solution is found. This approach is effective but falls short of what is typically expected of a physics analysis in at least three important ways. First, such calculations necessarily rely on an external tool to plot the trajectories and, therefore, outsources the physics analysis to someone else. Second, guess-and-check solutions typically require many iterations and are not very efficient, especially if one wants to examine a wide range of parameters. Third, when a solution is finally realized, one has no way of determining whether it is in any way ideal or optimal. In contrast, an analytic solution requires greater initial effort, but also rewards with physical insight and provides great flexibility to efficiently explore parameter dependency and the sensitivity of solutions to errors.

This paper proceeds with some preliminaries and a recap of important results in Sec. II, followed by a formal definition of the problem and derivation of the intercept condition in Sec. III, with a discussion of solutions in Sec. IV A and sensitivity of solutions in Sec. IV B. A brief analysis of the

rendezvous maneuver is covered in Sec. V with concluding thoughts presented in Sec. VI.

II. PRELIMINARIES

The overall goal of this work is to calculate the two thrusts that are required for: (a) interception (the meeting of spacecraft) and (b) rendezvous (the matching of speeds following interception). There exist multiple methods for calculating such maneuvers. References 6, 8, and 14 discuss a number of aspects of the intercept problem and its historical relevance. Reference 14, in particular, analyzes an intercept problem that is very similar to that discussed presently but in the rotating reference frame of the target and using small parameter expansions. The analysis presented here is different from these other analyses in that it views all motion in the planet's inertial frame, provides a method for exact solutions, and considers a constraint that is equivalent to a given quantity of fuel. This section begins by defining the coordinate system and initial conditions for this problem.

A. The coordinate system and initial conditions

The analysis presented here builds on that of Ref. 5 and uses the same coordinate system and symbolic representations. Figure 1 shows the coordinates used to describe the target and the chaser, the phase (ϕ) of the chaser's trajectory, and the two families of intercept solutions. Since intercepts can occur only where the two orbits intersect, the first family of intercept locations occurs at the chaser's initial position and the second family exists at an angle of 2ϕ, measured clockwise from this initial position.

The dynamic variables describing the positions of the craft will be identified using the subscripts: c for chaser, t for target, and i for initial conditions. Both craft begin on circular orbits of the same radius so that $r_{c,i} = r_{t,i} = r_0$, and the target will continue on this circular orbit after the chaser makes its intercept maneuver. The initial motion of both craft is taken to be counter-clockwise, which defines the sense of positive angular motion. The angular positions of the craft are measured relative to the initial position of the chaser; the target is initially separated from the chaser by a known angle, so that $\theta_{c,i} = 0$ and $\theta_{t,i} = \theta_0$. Angles in equations will be expressed in radians, whereas angles in subsequent figures will be expressed in degrees to aid in understanding.

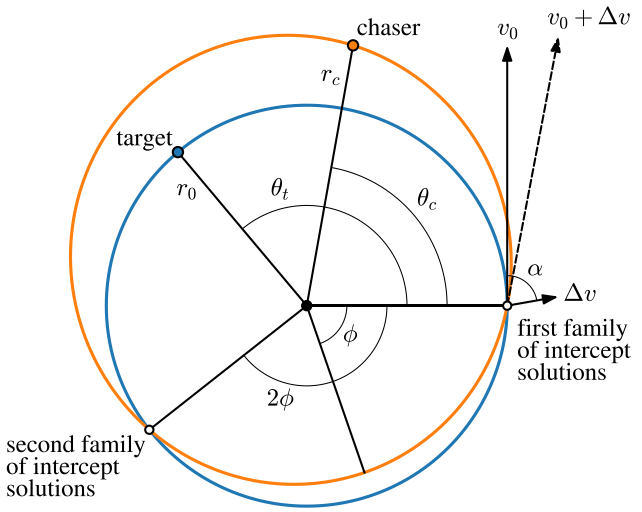

Fig. 1. The coordinate system used in this problem, showing the target with angular coordinate θ_t on a circular orbit of radius r_0. The chaser has radial coordinate r_c and angular coordinate θ_c at some time t following the intercept maneuver. The angular positions of all craft are measured counter-clockwise from the chaser's original position. The phase angle of the ellipse, ϕ, is the angle of the major axis of the chaser's elliptical orbit and is measured in the clockwise sense. The initial thrust vector of the chaser is shown at the right along with the resultant velocity vector.

Time is measured from the completion of the chaser's engine burn, which is modeled as being instantaneous so that the chaser's position at the start and end of the burn is $\theta_c = 0$. The orbital period of the target is $T_0 = 2\pi r_0/v_0$, with orbital frequency $\omega_0 = v_0/r_0$, where $v_0 = \sqrt{GM/r_0}$ is the linear speed of a craft on a circular orbit of radius r_0. Here, G is the universal gravitational constant, and M is the mass of the central gravitational body. The engine burn modifies the chaser's velocity by Δv directed at an angle of α clockwise from forward such that the radial and azimuthal components of the chaser's initial velocity are $v_{c,r,i} = \Delta v \sin(\alpha)$ and $v_{c,\theta,i} = v_0 + \Delta v \cos(\alpha)$, respectively. The normalized thrust is defined as $\delta = \Delta v/v_0$. A typical scale for many space missions is $\delta \approx 0.05$, but this can be greatly exceeded in special missions. For example, Ref. 14 presents a flight plan for the Apollo 11 mission wherein the third stage of the Saturn V rocket would use $\delta \approx 0.41$ to propel the lunar lander from Earth orbit to the moon.[15] In addition, normalized thrusts exceeding unity were achieved on the Voyager missions.

The following discussion refers to "fast-intercept" maneuvers, which are intercepts that occur before the target has completed a full orbit. Before completing an in-depth analysis, two predictions for fast-intercept maneuvers are made for the case where the target leads the chaser. First, it seems rather intuitive that a larger Δv should result in a smaller intercept time when the chaser is properly oriented (in the sense of Eq. (13)) for a fast-intercept maneuver. Therefore, as the impulse is increased, we anticipate that the angular coordinate at which intercept occurs should decrease. Second, thrusts that are directed purely forward will place the chaser in an orbit with a larger period and will only increase the distance between the craft. Instead, thrust maneuvers directed both forward and inward (with $270^\circ \leq \alpha < 360^\circ$) are likely candidates for fast-intercept solutions. While the overall orbital period after such a maneuver is longer than that of the target, such maneuvers work because the modified orbit initially takes the chaser to a lower altitude. Furthermore, an inward maneuver with some degree of reverse thrust ($180^\circ \leq \alpha \leq 270^\circ$) will also place the chaser onto a lower altitude orbit that will quickly advance the chaser's phase relative to the target. Therefore, we expect that fast-intercept maneuvers will require thrust angles between 180° and 360°. These predictions will be revisited in Sec. IV A when some sample solutions are examined.

B. The relationship between control parameters and trajectory parameters

Following the engine burn that propels it onto an intercept trajectory, the chaser will follow a path that is described by:

$$r_c(\theta_c) = r_0\left(\frac{1+\epsilon\cos(\phi)}{1+\epsilon\cos(\theta_c+\phi)}\right), \tag{1}$$

where ϵ is the eccentricity of the orbit and ϕ is the phase angle. Textbook descriptions of elliptical orbits typically

present this expression with the numerator being simply r_0. The modified form (1) is required so that the chaser has a radius of r_0 at $\theta_c = 0$, as required by the initial conditions.

The eccentricity ϵ and orbital phase angle ϕ can be related to the control parameters δ and α, as derived in the Appendix. These relationships are

$$\epsilon = \delta\sqrt{\sin^2(\alpha)(1+\delta\cos(\alpha))^2 + \cos^2(\alpha)(2+\delta\cos(\alpha))^2}, \tag{2}$$

and

$$\tan(\phi) = \tan(\alpha)\left(\frac{1+\delta\cos(\alpha)}{2+\delta\cos(\alpha)}\right). \tag{3}$$

When $\epsilon < 1$, the semi-major axis of the chaser's elliptical path is denoted as a. Then, the maximum radial excursion (apogee) is $(1+\epsilon)a$, which occurs when $\theta_c + \phi = \pi$. It follows from Eq. (1) that $a = r_0(1+\epsilon\cos(\phi))/(1-\epsilon^2)$. The period of the chaser's elliptical orbit can be calculated from Kepler's third law, $T_c^2 = (4\pi^2/GM)a^3$, and expressed in terms of problem parameters as

$$T_c = T_0\left(\frac{1+\epsilon\cos(\phi)}{1-\epsilon^2}\right)^{3/2}. \tag{4}$$

The normalized period (T_c/T_0) is plotted as a function of α in Fig. 2 for a range of δ. The orbital period relationship will enter the generalized intercept condition in Sec. III when accounting for the time required for the chaser to complete multiple orbits.

III. DERIVATION OF THE GENERALIZED INTERCEPT CONDITION

In general, the chaser could complete two thrust maneuvers. The first is the thrust required for interception, which is the condition that the chaser and target are coincident in space and time. The second is the thrust required for rendezvous, wherein the chaser matches the target's velocity. Obviously, the second maneuver would not be applicable in the case of an intentional collision, as with the DART mission. The thrust required for rendezvous is easily found once the intercept problem is solved. The interception problem is more difficult and is the focus of this section.

The intercept condition is determined as follows: Analysis of the radial coordinate determines where the orbits intersect, and therefore, the locations at which intercept can occur. The angular positions of the target and chaser are then expressed as functions of time. The intercept condition is found by requiring that the two craft have the same angular position (modulo 2π), which must also occur at one of the two points where the orbits intersect.

A. The radial intersection condition

While it is possible to draw an ellipse and a circle that intersect at four locations, the chaser's elliptical orbit can intersect the target's circular orbit at a maximum of two locations since the center of the target's orbit must coincide with one of the ellipse's foci, as illustrated in Fig. 1. This is readily proven by requiring the radial position of the chaser (r_c) be equal to that of the target (r_0) and solving for the angular position of the intersection, denoted as θ_x. Using Eq. (1) with $r_c = r_0$ provides the radial intersection condition $\cos(\theta_x + \phi) = \cos(\phi)$, from which two families of solutions emerge. The obvious solution that $\theta_x = 2\pi$ was the focus of the analysis in Ref. 5. The second intersection solution is

$$\theta_x = \begin{cases} 2\pi - 2\phi & 0 \le \phi < \pi, \\ 4\pi - 2\phi & \pi \le \phi < 2\pi, \end{cases} \tag{5}$$

where θ_x is limited to the range $[0, 2\pi)$. This expression for θ_x can be thought of as a function of ϕ or as a function of α (when δ is specified) through the relationship between ϕ and α described in Eq. (3). Both of these forms are shown in Fig. 3.

B. The angular equations of motion

Unlike the Lambert problem where time is an explicit constraint, time is not specified in this problem and will

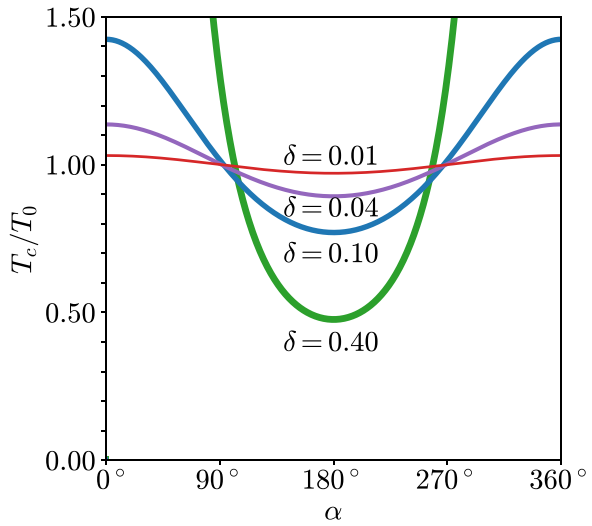

Fig. 2. The normalized orbital period of the chaser as a function of α calculated using Eq. (4). The maximum value of the normalized orbital period for a normalized thrust of $\delta = 0.40$ is about 125 at $\alpha = 0°$, corresponding to an eccentricity of 0.96, which shows that this case is approaching an unbound orbit.

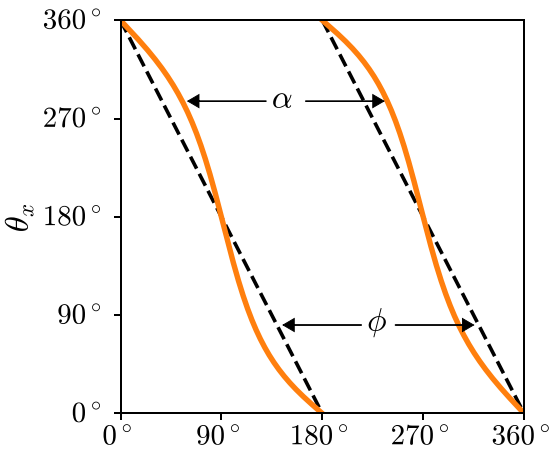

Fig. 3. The intersection angle of the two orbits, θ_x, is plotted against ϕ (black dashed) and α (solid orange) for the case of $\delta = 0.20$. The very weak dependence of ϕ on δ means that the θ_x vs α curves shown here can be taken as representative for a broad range of δ.

therefore be algebraically eliminated. As the target travels in uniform circular motion, its angular position evolves in time as

$$\theta_t(t) = \theta_0 + \omega_0 t. \tag{6}$$

There is no corresponding analytic expression for the chaser's angular position as a function of time. However, it is possible to describe the inverse relationship for the chaser (time as a function of the angular position). This relationship can be derived from the specific angular momentum of the chaser, $l_c = r_c^2\dot{\theta}_c$, which is a constant of the motion after the engine burn. This equation can be solved for time as a function of the chaser's angular position by expressing r_c in terms of θ using Eq. (1), separating the angular and time variables, and integrating between the initial and final coordinates. Doing so yields

$$t = T_0 \frac{(1+\epsilon\cos(\phi))^{3/2}}{2\pi}\int_0^{\theta_c} \frac{d\theta}{(1+\epsilon\cos(\theta+\phi))^2}, \tag{7}$$

where the expression has been simplified using $\omega_0 = v_0/r_0$ and $l_c = r_0 v_0 (1+\epsilon\cos(\phi))^{1/2}$, which is an alternate form for l_c that is presented in Eq. (A6) of the Appendix. Critically, the chaser's angular position appears as the upper limit of the integral. This result is valid for any final angle and for any values of ϵ and ϕ, which means that parabolic and hyperbolic paths are also potential intercept trajectories.

Evaluated at $\theta_c = 2\pi$, the integral in Eq. (7) is equal to $2\pi/(1-\epsilon^2)^{3/2}$, which reproduces the chaser's orbital period given in Eq. (4). If the chaser completes more than one orbit, its angular coordinate can be expressed as $\theta_c = 2\pi n_c + \theta_c'$, where $n_c \in \mathbb{N}$ counts the number of whole orbits and $\theta_c' \in [0, 2\pi)$. Therefore, the time required to travel the total angular distance is then n_c times the orbital period plus the remainder described in Eq. (7) evaluated at θ_c'. That is,

$$t = n_c T_c + \frac{1}{\omega_0}(1+\epsilon\cos(\phi))^{3/2} \times \int_0^{\theta_c'} \frac{d\theta}{(1+\epsilon\cos(\theta+\phi))^2}. \tag{8}$$

The integral can be evaluated numerically or analytically.[3,16,17] The analytic solution is presented here for the sake of completeness. Defining the second term on the RHS of Eq. (8) as $I(\theta_c';\epsilon,\phi)/\omega_0$, the analytic expression for this integral is

$$I(\theta_c';\epsilon,\phi) = \left(\frac{1+\epsilon\cos(\phi)}{1-\epsilon^2}\right)^{3/2}\left[q(\theta_c'+\phi) - q(\phi)\right], \tag{9}$$

where the new quantity, q, is given by

$$q(z) = \psi(z) - \epsilon\sin(\psi(z)), \tag{10}$$

which itself depends on another quantity ψ,

$$\psi(z) = 2\tan^{-1}\left(\sqrt{\frac{1-\epsilon}{1+\epsilon}}\tan\left(\frac{z}{2}\right)\right). \tag{11}$$

Equations (9)–(11) are collectively known as Kepler's equation. They have the advantage that they do not require any numerics, but they are rather complicated and their physical origin is not very transparent. When using these equations, care must be taken to enforce continuity in ψ as the inverse tangent function jumps between $+\pi/2$ and $-\pi/2$ when z passes through π. Additionally, the RHS of Eq. (8) is described using only $I(\theta_c';\epsilon,\phi)$ so that readers may use their preferred method for evaluating the integral.

As was done for the chaser, the angular position of the target can be described as a multiple of 2π plus a remainder using $\theta_t = 2\pi n_t + \theta_t'$, where $n_t \in \mathbb{N}$ and $\theta_t' \in [0, 2\pi)$. Using this form for the angular position of the target and eliminating time in Eq. (6) by replacing it with the RHS of Eq. 8 gives

$$2\pi n_t + \theta_t' = \theta_0 + n_c\omega_0 T_c + I(\theta_c';\epsilon,\phi). \tag{12}$$

This equation describes the angular position of the target as a function of the angular position of the chaser.

C. The intercept condition

The intercept condition is realized when the angular coordinates of the target and chaser are the same and also at an orbital intersection point, that is, $\theta_t' = \theta_c' = \theta_x$. Imposing these constraints in Eq. (12) yields the generalized intercept condition,

$$2\pi n_t + \theta_x = \theta_0 + n_c\omega_0 T_c + I(\theta_x;\epsilon,\phi). \tag{13}$$

It is important to note that, unlike Eq. (12) which is true for any values of α and δ, Eq. (13) is true only for particular values of these parameters, since intercept requires precision coordination of the target and chaser. The intercept problem is solved with the discovery of particular values of α and δ that satisfy Eq. (13). In analyzing this problem, it must be recalled that ϵ and ϕ are functions of α and δ through Eqs. (2) and (3), respectively, and θ_x is a function of ϕ through Eq. (5).

We briefly pause to consider how Eq. (13) should be interpreted. The origin of this equation is Eq. (6), which describes the angular position of the target as a function of time. The second and third terms on the RHS of Eq. (13) represent the time (multiplied by ω_0) required for the chaser to travel to an intersection point of the orbits. Therefore, the RHS represents *the actual angular position of the target when the chaser is at an orbital intersection point* θ_x. The LHS should be interpreted as *the goal of having the target also at the same intersection point*. It is worth noting that limiting the solution space to $\theta_x = 0$ eliminates the second term on the LHS and the integral term on the RHS, which reproduces Eq. (18) of Ref. 5 that describes the intercept condition for the first family of solutions.

IV. SOLUTIONS FOR THE SECOND FAMILY OF INTERCEPT LOCATIONS

This search for intercept solutions proceeds by treating α as the sole unknown control parameter, taking the normalized thrust, δ, as specified. Phrased as a question, the intercept condition asks "For what values of α is Eq. (13) true when δ is specified?" Due to the transcendental nature of Eq. (13), solutions cannot be found analytically; they can be found by scanning through all possible values of α and identifying those values which satisfy Eq. (13).

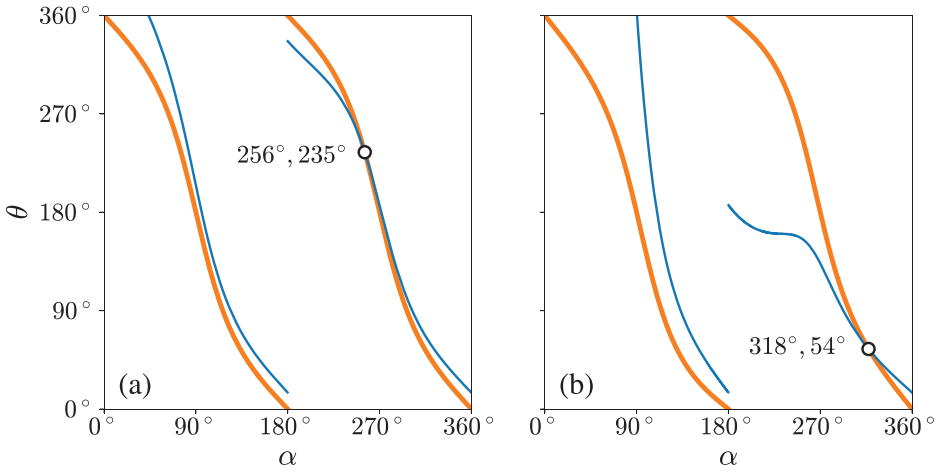

Fig. 4. The thick orange curves represent the LHS of Eq. (13), and the thin blue curves represent the RHS of that equation for (a) $\delta = 0.04$ and (b) $\delta = 0.40$. The initial angular separation is $\theta_0 = 15^\circ$ in both cases. The numerical values next to each crossing identify (α, θ): the thrust angle which solves the fast-intercept problem, and the angle at which intercept occurs.

A. Intercept solutions

Figure 4 presents two fast-intercept solutions ($n_c = n_t = 0$) for $\delta = 0.04$ and $\delta = 0.40$, as representative cases. The normalized thrust used in the second case should be considered a strong thrust as it is close to the limit $\delta_{\text{escape}} = \sqrt{2} - 1 \approx 0.41$ for escape from orbit due to a forward thrust maneuver. Both cases assume initial conditions where the target leads the chaser ($\theta_0 > 0$), though it should be noted that negative values of θ_0 would also be perfectly acceptable. The thin blue curves in Fig. 4 represent the RHS of Eq. (13), the actual position of the target when the chaser is located at a crossing of the orbits (θ_x). The thick orange lines represent the LHS of Eq. (13), the angular location of the orbital intersection. Notably, it seems that these fast-intercept solutions require $\alpha > 180^\circ$, and it is clear that larger values of δ achieve intercept more quickly (in agreement with the predictions of Sec. II A). The trajectories for these two fast-intercept solutions are presented in Fig. 5. Notably, the second solution with $\delta = 0.40$ will grossly overshoot the target if there is not a rendezvous maneuver or collision with the target.

Figure 6 illustrates the solution space for the generalized intercept condition when $\delta = 0.39$ and $\theta_0 = 15^\circ$, allowing for multiple orbits of the chaser and target. The value of $\delta = 0.39$ was chosen for its relevance to the sensitivity analysis discussed in Sec. IV B. Intercept solutions with θ in the range of 0°–360° are the fast-intercept solutions with $n_t = 0$, whereas those above 360° are multi-orbit solutions with $n_t = 1$. Table I lists the numerical values for these intercept solutions.

B. Sensitivity to variations in α

Trajectory corrections are almost always needed in real missions to compensate for guidance errors, mechanical inaccuracies, and measurement uncertainties. A trajectory is considered efficient and stable as long as required corrections are much smaller than primary mission maneuvers. The Cassini–Huygens mission, for example, was designed with a deep-space maneuver (DSM) Δv of approximately 450 m/s, along with many smaller trajectory correction maneuvers (TCMs), all of which were less than 10% of the primary thrust.[18] The use of small corrections is only possible when the trajectories are relatively insensitive to errors in the initial thrust vector.

The following sensitivity analysis considers only the effect of variations in the angular control variable, α, though a

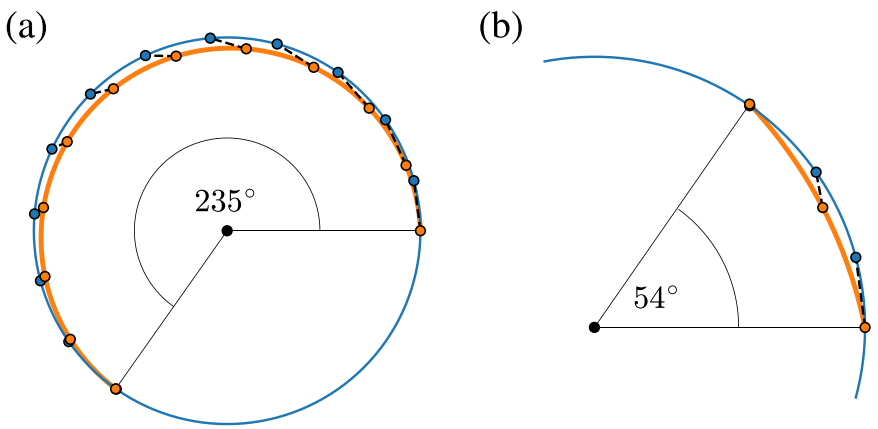

Fig. 5. Strobe-effect illustration of the trajectories of the chaser (orange, thick) and the target (blue, thin), plotted at 20° increments of the target, for the intercept solutions identified in Fig. 4 for (a) $\delta = 0.04$ and (b) $\delta = 0.40$. The black dotted line between the points identifies position pairs at equal intervals of time. The black dots interior to the orbits identify the center of force.

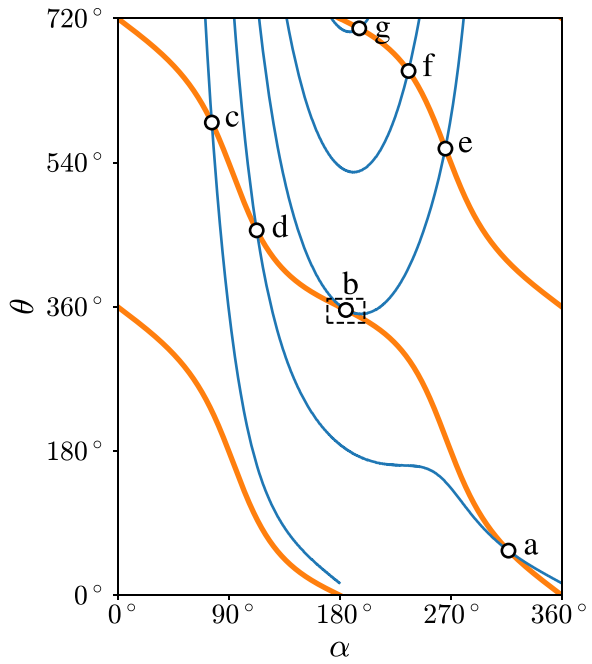

Fig. 6. The thick orange curves represent the LHS of Eq. (13), and the thin blue curves represent the RHS of that equation for $\delta = 0.39$ and $\theta_0 = 15°$. The points labeled a–g are all possible solutions occurring before the target has completed two full orbits. The dashed box indicates the parameter range shown in Fig. 7.

similar analysis could be conducted for variations in δ. With the first family of intercept solutions analyzed in Ref. 5, it was straightforward to search for optimal (stable) solutions because α only appeared in the RHS of the intercept condition. Proving the existence of stable solutions amounted to showing that, for some intercept solutions, the derivative of the RHS of the intercept condition with respect to α is zero. This led to the conclusion that perfectly forward or reverse thrusts are optimal for this first family of solutions.

For the generalized intercept condition, an analytic treatment of stability is much more difficult on account of the many ways in which both the LHS and RHS of Eq. (13) depend on α. Instead of mathematically proving the existence of stable solutions, the intercept solutions identified in Fig. 6 are inspected for their sensitivity to small variations in α. In particular, the boxed region in Fig. 6 is expanded in Fig. 7, showing that the two curves are tangent to each other for intercept solution *b*. Thus, the existence of stable solutions for the generalized intercept condition is proved via example, though it is not yet known whether stable, fast-intercept solutions exist.

Table I. List of numerical values for the solutions presented in Fig. 6.

Figure 6 tag	n_t	n_c	α	θ_x	θ_t	θ_c
a	0	0	317°	56°	56°	56°
b	0	1	186°	355°	355°	715°
c	1	0	76°	230°	590°	230°
d	1	1	113°	95°	455°	455°
e	1	1	266°	198°	558°	558°
f	1	2	236°	295°	655°	1015°
g	1	3	196°	348°	708°	1428°

Stability analysis must also take into account the steepness of the curves' slopes in the vicinity of the solution. As an example, assume that a mission can tolerate a deviation of 1° between the positions of the craft. Figure 7 shows that a 1° output error arises from a ±5° input error for this solution, corresponding to a sensitivity ratio (output variation/input variation) of about 0.2. In contrast, intercept solutions *c*–*g* from Fig. 6 have sensitivity ratios of order 10 and would, therefore, be unlikely candidates for an intercept mission. Interestingly, solution *a* has an impressive sensitivity ratio of about 0.5 despite the fact that the curves are not tangent at the solution point, a result of the relatively weak gradients in this vicinity. Even if the curves cross, low-sensitivity solutions can still arise if the crossing is near one curve's inflection point as in Fig. 4(a).

V. RENDEZVOUS

The thrust required for rendezvous can be derived from the equations of motion or from symmetry arguments, both of which are described here. The chaser's velocity components are given in Eqs. (A1) and (A2) from the Appendix. Evaluating the azimuthal velocity component at the intersection angle described in Eq. (5) results in $v_{c,\theta} = v_0 + \Delta v \cos(\alpha)$, which is the same as the initial state. Evaluation of the radial component of velocity gives $v_{c,r} = -\Delta v_0 \sin(\alpha)$, which means that the radial velocity at interception is exactly opposite to the initial radial velocity. The same conclusion can be surmised from the symmetry of the problem using Fig. 1, where the velocity components have the same magnitude and the radial component must have changed sign. It follows that the rendezvous maneuver at the second family of intercept locations requires a thrust of magnitude Δv directed at an angle of $\pi - \alpha$.

VI. CONCLUSIONS

Implementing a fuel constraint (a specified Δv) in the intercept problem offers pedagogical advantages compared to the Lambert problem: a constant magnitude thrust vector with a variable direction is easier to visualize than the fixed time-to-interception formulation. The analysis presented in

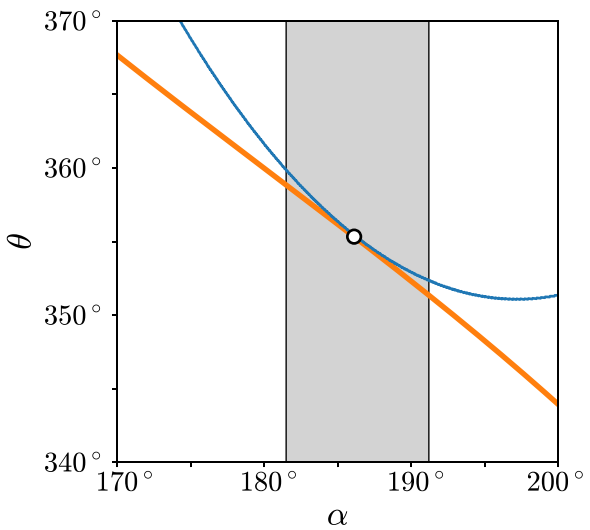

Fig. 7. Intercept solution *b* identified in the dashed box of Fig. 6. The gray bands identify the range of α for which the target and chaser have an angular separation of 1° or less around the ideal intercept location, resulting in an allowable uncertainty on α of about 5°.

this work extends the intercept problem that was introduced in Ref. 5 by analyzing solutions occuring at the second family of intersection locations. The culmination of this work is Eq. (13), which is the most general statement of the intercept condition for this problem.

In addition to presenting a general intercept condition that allows intercept locations to be calculated, this work has shown how fast-intercept solutions (occurring before the target has completed one full orbit) can be calculated. The existence of solutions that are stable with respect to variations in α was proven through an example with $\delta = 0.39$ and $\theta_0 = 15^\circ$. It is not known whether there exist low-sensitivity fast-intercept solutions or whether there exist intercept solutions that are simultaneously insensitive to variations in both α and δ. There are, of course, many other rich and challenging problems that could be further examined using the framework and analytical methods described here, including a mathematical expression for the stability of solutions to the generalized intercept condition, the existence of low-sensitivity fast-intercept maneuvers, initial orbits that are not circular, and initial conditions that are not co-orbital.

AUTHOR DECLARATIONS

Conflict of Interest

The authors have no conflicts to disclose.

APPENDIX: DERIVATION OF THE EQUATIONS FOR ϵ AND ϕ

This derivation of the equations for ϵ and ϕ in terms of the control parameters, δ and α, follows the logic presented in Ref. 5. Two equations of constraint are developed and merged to derive these key relationships. One constraint emerges from kinematics and angular momentum, and the other from conservation of total energy. At $t = 0$, after the engine burn has been completed, the mass, angular momentum, and total energy of the chaser are constants of the motion. Since any function of these quantities must also be a constant of the motion, the following analysis considers the specific angular momentum and the specific total energy, being the angular momentum and total energy divided by the mass. The specific angular momentum is $l_c = r v_\theta$. Referring to the velocity components described in Fig. 1, it follows that $l_c = r_0\, v_0(1 + \delta\cos(\alpha))$ immediately after the engine burn has concluded. This constant of the motion can be used with Eq. (1) to solve for the azimuthal velocity through $v_\theta = l_c/r$, which gives

$$v_{c,\theta} = v_0(1 + \delta\cos(\alpha))\frac{1 + \epsilon\cos(\theta_c + \phi)}{1 + \epsilon\cos(\phi)}. \tag{A1}$$

An expression for the radial velocity can be derived using the chain rule in Eq. (1), $v_r = (dr/d\theta)\dot{\theta} = (dr/d\theta)(v_\theta/r)$, together with the prior result to give

$$v_{c,r} = v_0(1 + \delta\cos(\alpha))\frac{\epsilon\sin(\theta_c + \phi)}{1 + \epsilon\cos(\phi)}. \tag{A2}$$

The first constraint is found by taking the ratio of the radial and azimuthal velocities, using Eqs. (A2) and (A1), and equating this to the ratio of velocities from the initial conditions as depicted in Fig. 1. This yields

$$\frac{\epsilon\sin(\phi)}{1 + \epsilon\cos(\phi)} = \frac{\delta\sin(\alpha)}{1 + \delta\cos(\alpha)}. \tag{A3}$$

The second constraint results from consideration of the specific total energy of the chaser, $e_c = \frac{1}{2}(v_{c,r}^2 + v_{c,\theta}^2) - GM/r$, which can be calculated using the prior results. Noting that Newton's second law analyzed for the target on its circular orbit gives $GM = r_0 v_0^2$, we have

$$e = \frac{1}{2}\frac{v_0^2}{(1 + \epsilon\cos(\phi))^2}\left[\epsilon^2 - 1 + 2\epsilon((1 + \delta\cos(\alpha))^2 - (1 + \epsilon\cos(\phi)))\cos(\theta + \phi)\right]. \tag{A4}$$

Equation (A4) must actually be independent of angle in order for e to be a constant of the motion. Therefore, the coefficient of the $\cos(\theta + \phi)$ must be identically zero. This yields the second constraint,

$$1 + \epsilon\cos(\phi) = (1 + \delta\cos(\alpha))^2. \tag{A5}$$

This result also allows the specific angular momentum of the chaser to be expressed as

$$l_c = r_0 v_0(1 + \epsilon\cos(\phi))^{1/2}. \tag{A6}$$

Finally, the two constraints, Eqs. (A3) and (A5), can be combined to solve for ϵ and ϕ. These expressions are

$$\epsilon = \delta\sqrt{\sin^2(\alpha)(1 + \delta\cos(\alpha))^2 + \cos^2(\alpha)(2 + \delta\cos(\alpha))^2}, \tag{A7}$$

and

$$\tan(\phi) = \tan(\alpha)\frac{1 + \delta\cos(\alpha)}{2 + \delta\cos(\alpha)}. \tag{A8}$$

Useful reference points for characterizing the scale of ϵ are its minimum and maximum values. The minimum of Eq. (A7) is $\epsilon = \delta$, which occurs at $\alpha = 90^\circ$ and 270°. A maximum of $\epsilon = \delta(2 + \delta)$ occurs at $\alpha = 0^\circ$ and 180°. It was shown in Ref. 5 that ϕ has very weak dependence on δ, such that the approximation $\tan(\phi) = \frac{1}{2}\tan(\alpha)$ is accurate to within 0.5° for $\delta \leq 0.05$.

[a]Electronic mail: eric.edlund@cortland.edu, ORCID: 0000-0001-5320-4996.

[1]J. L. Lagrange, *Mécanique Analytique, Vol. II* (Académie des Sciences, Paris, 1788).
[2]C. F. Gauss, *Theory of the Motion of the Heavenly Bodies Moving about the Sun in Conic Sections: A Translation of Gauss's "Theoria Motus"* (Little, Brown and Co., Boston, MA, 1857).
[3]I. R. Gatland, "Gravitational orbits and the Lambert problem," Am. J. Phys. **90**(3), 177–178 (2022).
[4]A. M. Capece and J. L. Gazley, "The Hohman transfer as an application for teaching introductory physics," Am. J. Phys. **89**(11), 1002–1008 (2021).
[5]B. W. Carroll, "The delicate dance of orbital rendezvous," Am. J. Phys. **87**(8), 627–637 (2019).
[6]P. R. Blanco and C. E. Mungan, "High-speed escape from a circular orbit," Am. J. Phys. **89**(1), 72–79 (2021).
[7]R. W. Easton, R. L. Anderson, and W. Lo, "Conic transfer arcs for Kepler's problem," Am. J. Phys. **90**, 666–671 (2022).
[8]E. M. Edlund, "Interception and rendezvous: An intuition-building approach to orbital dynamics," Am. J. Phys. **89**, 559–566 (2021).

[9]L. M. Smallwood, D. M. Katz, and M. W. Richmond, "Near earth objects: A brief review and a student project," Am. J. Phys. **72**(2), 264–279 (2004).
[10]NASA, "Planetary defense coordination office," 2022. <https://www.nasa.gov/planetarydefense/overview>
[11]A. F. Chang, A. S. Rivkin, P. Michel, J. Atchison, O. Barnouin, L. Benner, N. L. Chabot, C. Ernst, E. G. Fahnestock, M. Keuppers, P. Pravec, E. Rainey, D. C. Richardson, A. M. Stickle, and C. Thomas, "AIDA DART asteroid deflection test: Planetary defense and science objectives," Planet. Space Sci. **157**, 104–115 (2018).
[12]T. Pultarov, "Astroscale's space junk removal satellite aces 1st orbital test," 2021. <https://www.space.com/astroscale-first-space-junk-capture-demonstration>
[13]W. J. Hennigan, "Exclusive: Strange Russian spacecraft shadowing U.S. spy satellite, general says," 2020. <https://time.com/5779315/russian-spacecraft-spy-satellite-space-force/>.
[14]L. J. Riché, G. M. Colton, and T. A. Guillory, "Apollo 11 flight plan," *NASA* (1969). <https://www.hq.nasa.gov/alsj/a11/a11fltpln_final_reformat.pdf>
[15]The NASA report on the Apollo 11 flight plan (Ref. 14) calls for an initially circular orbit at an altitude of 100 nautical miles, and a Δv for the trans-lunar injection (TLI) maneuver of 10 451 feet per second. These values provide an estimate of $\delta \approx 0.409$, assuming an optimal escape maneuver using a forward thrust at $\alpha = 0°$.
[16]H. Goldstein, C. P. Poole, and J. Safko, *Classical Mechanics* (Pearson, London, 2011).
[17]H. D. Curtis, *Orbital Mechanics for Engineering Students* (Elsevier, Amsterdam, 2014).
[18]T. Goodson, B. Buffington, Y. Hahn, N. Strange, S. Wagner, and M. Wong, "Cassini-Huygens maneuver experience: cruits and arrival at Saturn," *AASI-AIAA Astrodynamics Specialist Conference* (AIAA, Reston, VA, 2005), p. AAS 05-286.

Drury University Laboratory

Drury University in Springfield, Missouri dates from1873. This picture was taken in the physics laboratory about the start of the twentieth century. The table on the right-hand holds a Wimshurst electrostatic machine with twenty inch ebonite disks; this could be used to activate discharge tubes as well as the new cold-cathode x ray tubes. A large calorimeter is also on the table. In the background is an Atwood's machine. (Picture and text by Thomas B. Greenslade, Jr., Kenyon College)